

Experimental Study of Quantum Structures in Solids*

Kaare J. Nygaard

Electronic Structure of Materials Centre,
Flinders University of South Australia,
Bedford Park, S.A. 5042, Australia.

Abstract

The object of the experiment is to measure electron binding energy spectra in solids at a series of selected bound electron momenta. The present apparatus is based on developments in atomic and molecular spectroscopy and uses a 10 keV electron beam incident on a thin (80 Å) amorphous carbon film. The exit electrons in the (e,2e) reaction are studied in a symmetric coplanar geometry using hemispherical analysers and position-sensitive detectors. The resultant coincidence count rate is proportional to the probability of finding a target electron with a given binding energy and momentum. Data were obtained with binding energies from 0 to 40 eV with momentum as parameter. Contributions from the π and σ bands are clearly demonstrated. Future investigations in a new experimental system will be devoted to single crystals of metals, semiconductors and macro-molecules.

1. Introduction

The periodic structure of ions in a crystal lattice gives rise to potentials and wavefunctions capable of describing electron densities and momenta within certain energy bands $\epsilon_i(\mathbf{k})$. In momentum space, the probability density of finding an electron with binding energy ϵ_i and momentum \mathbf{k} is given by $|\phi_i(\mathbf{k})|^2$, where $\phi_i(\mathbf{k})$ is the momentum-dependent wavefunction. The salient feature of electron momentum spectroscopy (EMS) is that a quantity proportional to $|\phi_i(\mathbf{k})|^2$ can be experimentally determined. On the other hand, the position-dependent probability density $|\psi_i(\mathbf{r})|^2$ is non-empirical. In principle, if one of the wavefunctions $\phi_i(\mathbf{k})$ or $\psi_i(\mathbf{r})$ is known, the other can be determined by a Dirac-Fourier transformation. The probability density $|\phi_i(\mathbf{k})|^2$ is sometimes called the 'momentum probability distribution' or simply 'momentum distribution' or 'spectral momentum density'.

The method of EMS is based on the (e, 2e) technique, in which a beam of monoenergetic electrons of energy E_0 and momentum \mathbf{p}_0 is incident upon a target. Investigations of atoms and molecules have been reviewed in recent articles by McCarthy and Weigold (1988) and Weigold (1991, present issue p. 277). Subsequently, it was a natural extension to apply the previously developed experimental and theoretical methodologies to the realm of solids and surfaces.

* Dedicated to Professor Ian McCarthy on the occasion of his sixtieth birthday.

Consider initially a single target electron with binding energy ϵ_i and momentum \mathbf{k} . The problem at hand is to determine both ϵ_i and \mathbf{k} experimentally, not only for a single particle, but for an ensemble of electrons. This is accomplished by observing a multitude of specific (e, 2e) collision events. A specific event is characterised by

$$E_0 = E_A + E_B - \epsilon_i, \quad (1)$$

where the two outgoing electrons of energy E_A and E_B are detected in coincidence to ensure that they originate from the same event. Conservation of momentum for the unique event under scrutiny is prescribed by

$$\mathbf{p}_0 + \mathbf{k} = \mathbf{p}_A + \mathbf{p}_B, \quad (2)$$

where \mathbf{p}_A and \mathbf{p}_B are the momenta of the two exit electrons. Since the dynamic conditions of all (e, 2e) reactions are completely known, binding energies and momenta for an ensemble of electrons in a solid material can be determined. Furthermore, the probability density of finding electrons with binding energy ϵ_i and momentum \mathbf{k} within a certain band is mapped out by determining the cross section (McCarthy and Weigold 1988).

The material in this essay is organised as follows: in Section 2 a special geometry which permits detection of target electrons for ranges of momentum and binding energy values is developed. The experimental procedure is described in Section 3, followed by a presentation of results in amorphous carbon (Section 4) and conclusions (Section 5).

2. Geometrical Considerations

The momentum transferred by the incident electron in the (e, 2e) reaction can be written as

$$\mathbf{K} = -\mathbf{k} + \mathbf{p}_B,$$

where, for free atoms and molecules, $-\mathbf{k}$ is the momentum transferred to the ion left behind. In solids, $-\mathbf{k}$ represents the momentum imparted to the crystal lattice. It is customary to let \mathbf{p}_B be the momentum of the 'ejected' electron and \mathbf{p}_A the momentum of the 'scattered' electron.

In the coplanar geometry which will be treated next, the momentum transfer $|\mathbf{K}|$ is maximised for any after-collision energy $E = E_A + E_B$, if $\theta_A = \theta_B = 45^\circ$ relative to the direction of the high energy incident electron. The momentum transfer is also independent of the azimuthal angle ϕ , which may be varied to obtain the momentum profile. Equivalently, it is possible to establish a momentum range by observing the two exit electrons in the same plane by imposing a small energy asymmetry ΔE while maintaining $(E_A + E_B)$ constant. This is achieved by letting

$$E_{A,B} = \frac{1}{2}(E_0 + \epsilon_i) \pm \Delta E \quad (3)$$

and scanning in ΔE . Then, in atomic units, we have

$$|\mathbf{p}_{A,B}| = \sqrt{2} \left[\frac{1}{2}(E_0 + \epsilon_i) \pm \Delta E \right]^{\frac{1}{2}} \approx |\mathbf{p}| \pm |\Delta \mathbf{p}_{A,B}| \quad (4)$$

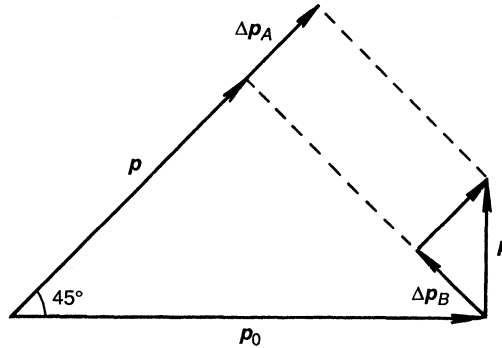


Fig. 1. Diagram for determining bound electron momentum \mathbf{k} in the symmetric coplanar geometry according to equation (5).

where $p^2 = p_0^2/2$. Fig. 1 shows that

$$|\mathbf{k}|^2 = |\Delta\mathbf{p}_A|^2 + |\Delta\mathbf{p}_B|^2 \quad (5)$$

and that the target momentum direction available for study is perpendicular to the incident electron beam. A simple calculation gives

$$|\mathbf{k}| = |\mathbf{p}_0| \frac{\Delta E}{E_0} \left(1 + \frac{\epsilon_i}{E_0}\right). \quad (6)$$

In the experiment, the binding energy correction is 0.2% for $\epsilon_i = 20$ eV and $E_0 = 10000$ eV and will subsequently be neglected. The obvious advantage of this method is that a range of target momenta perpendicular to the incident beam and in the collision plane can be studied by varying $\Delta E/E_0$ without changing the position of any of the analysers. On the other hand, momentum components parallel to the beam can be analysed for polar angles slightly different from 45° by using electrostatic deflection of the exit electrons (Ritter *et al.* 1984a). In amorphous and partially amorphous films we expect little difference between electron momentum densities observed in the directions discussed above.

3. Experimental

A schematic diagram of the apparatus based on the coplanar geometry is shown in Fig. 2. The thin film target, which is located at ground potential, is bombarded by electrons of energy 10 keV. In order to establish the momentum selection scheme discussed above, the two analysers are floating at different voltages $-(\frac{1}{2}V_0 \pm \Delta V)$ relative to ground. The analyser entrance slits define an overall momentum resolution of about 0.1 atomic unit ($1a_0^{-1} = 1.89 \text{ \AA}^{-1}$). The energy resolution of the apparatus is better than 2 eV. Each analyser comprises a retarding and focussing lens system, a hemispherical energy dispersion element and a multichannel plate/resistive anode detector. These are similar to those discussed by McCarthy and Weigold (1988).

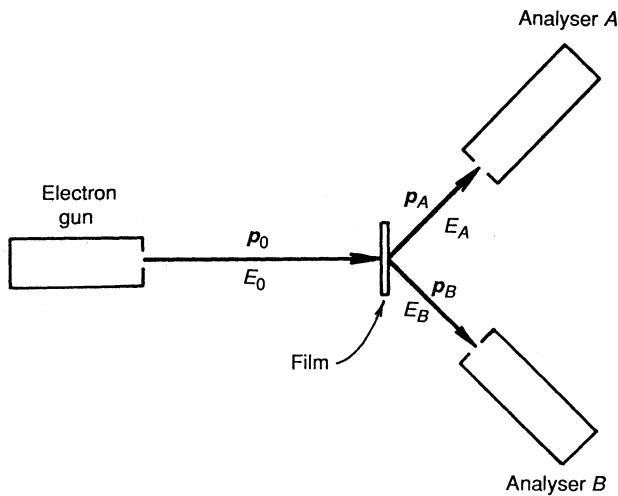


Fig. 2. Schematic diagram of symmetric coplanar apparatus. The two analysers are floating at different potentials relative to ground to establish desired momentum values.

Briefly, the 'fast' pulses from the back of the two channel plates are counted in coincidence by a time-to-amplitude converter. The details of the timing and energy analyses are similar to the technique described in a recent paper by Lower and Weigold (1989). Two separate single channel analysers are employed to define the coincidence and background windows; the background window is about 15 times wider than the signal window in order to reduce the statistical error in background subtraction. The energies of the two exit electrons are measured by the 'slow' pulses extracted from the two resistive anodes in such a way that $(E_A + E_B)$ is always constant (Weigold *et al.* 1991).

The experiment is controlled by an IBM PC equipped with a multichannel analyser for data acquisition and monitoring purposes. The computer increments the energy of the incident electrons and adjusts the floating analyser voltages by an amount $\pm \Delta V$ as required to select the desired momentum value. Finally, the accumulated coincidence counts, properly corrected for background events, are displayed as a function of binding energy.

4. Results and Discussion

The data to be presented in this report were obtained under the following experimental conditions: the incident electron energy was 10 keV with a beam current of $3.5 \mu\text{A}$ which stayed constant within $\pm 1\%$ for several weeks. The position of the binding energy range was adjusted to cover 8 eV above and 37 eV below the Fermi energy ϵ_F . The electron beam energy was incremented in amounts of 0.7 eV. Data accumulation time to obtain one energy loss spectrum at a fixed momentum value was about 72 hours. The sample studied was an 80 Å thick amorphous carbon film manufactured by the Arizona Carbon Foil Company. The film was free-standing over an aperture of 2 mm diameter. Typical data are displayed in Fig. 3. The spectral density for $k = 0$ shows a distinct peak at 21 eV at the $k = 0$ location of one of the σ bands. The

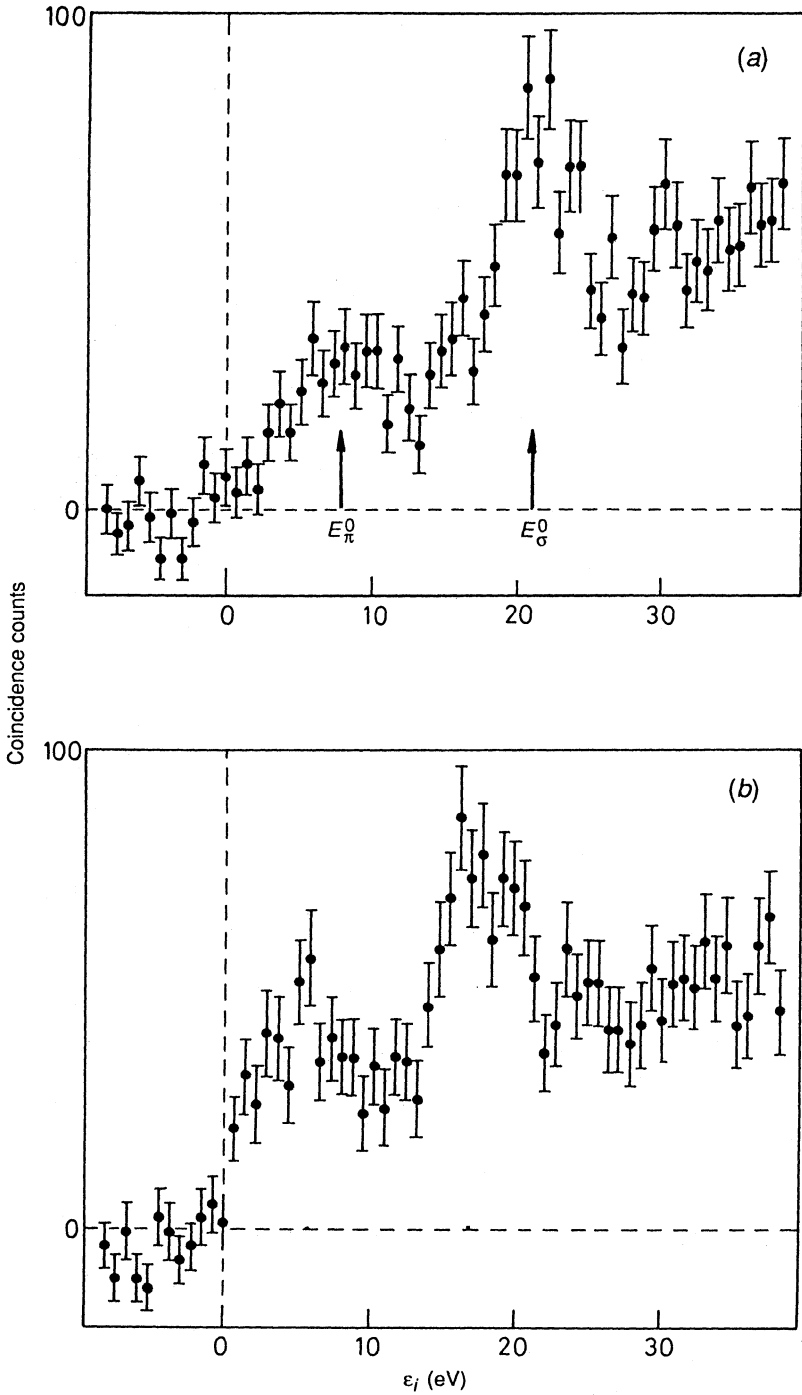


Fig. 3. Accumulated coincidence counts (arbitrary scale) for (a) $k=0$ and (b) $k=0.4a_0^{-1}$ in an amorphous carbon film 80 Å thick. The incident electron beam energy was 10 keV.

structure at lower energy is ascribed to ionisation of π electrons. Notice that there are no coincidence counts above ϵ_F to within two mean standard deviations (two error bars). The counts appearing beyond 25 eV are partly due to plasmon losses and can be corrected by a deconvolution process developed by Jones and Ritter (1986).

Comparison with the results for $k = 0.4a_0^{-1}$ (Fig. 3b) reveals some striking differences: firstly, the peak position of the σ band has been displaced in the direction of the Fermi energy by an amount of 5 eV while the probability density of this structure has hardly changed. Secondly, the broader structure previously ascribed to π electrons has increased significantly in magnitude and is shifted closer to the Fermi energy with a well defined onset at this energy. Thirdly, the coincidence count rates for energies beyond 30 eV for both $k = 0$ and $k = 0.4a_0^{-1}$ are the same within the experimental accuracy. In general, the results are similar to those reported on amorphous carbon by Ritter *et al.* (1984b) who discuss the same bands, but with an energy resolution of only 6 eV FWHM.

It may be surprising that any structure at all is seen in amorphous carbon. Experimentally, it has been observed that the amorphous film becomes more graphitic due to electron bombardment. In the present experiment, the films have been aged by electron bombardment for a few days until the shape of the $k = 0$ spectrum becomes constant. On theoretical grounds (Ziman 1971) it has been suggested that for small k -values an amorphous film exhibits graphitic behaviour. In that case, the electron spectral densities are expected to be similar to an angular average of the spectral densities in crystalline graphite (Gao *et al.* 1988). The ratio between graphitic and diamond-like bonds cannot be ascertained from the present data.

5. Conclusions

The present investigation has demonstrated the feasibility of conducting (e, 2e) experiments in solids with momentum and energy resolutions of $0.1a_0^{-1}$ and 2 eV, respectively. Data obtained in thin carbon films demonstrate a strong dispersion of the σ band and an increased probability of ionising π electrons as the momentum of the bound electrons is increased from 0 to $0.4a_0^{-1}$. The apparatus is configured in the symmetric coplanar geometry using two identical hemispherical analysers with one-dimensional energy dispersion and detectors. Under typical operating conditions, the maximum coincidence count rate is 5 per min. The time needed to accumulate a set of binding energy spectra covering ten different momentum values would be as high as 30 days.

In the future, we plan to study properties of metals, semiconductors, superconductors and macro-molecules. A new spectrometer operating at higher electron beam energies, much higher count rates and with better energy resolution is presently being developed and will be used in these investigations.

Acknowledgments

This essay is dedicated to I.E. McCarthy to recognise his contributions to many areas of physics, among them theories designed to create a deeper understanding of 'life in momentum space'. The author acknowledges the research conducted over a number of years by E. Weigold in developing

electron momentum spectrometers for investigating atoms and molecules and for his vision in establishing the Electronic Structure of Materials Centre at The Flinders University of South Australia. Finally, I gratefully acknowledge the many contributions made to this work by J. Lower, Y. Chen, M. Bharathi, A.L. Ritter and L. Frost.

References

- Gao, C., Ritter, A.L., Dennison, J.R., and Holzwarth, N.A.W. (1988). *Phys. Rev. B* **37**, 3914.
Jones, R., and Ritter, A.L. (1986). *J. Elect. Spectrosc. Related Phenomena* **40**, 285.
Lower, J., and Weigold, E. (1989). *J. Phys. E* **22**, 421.
McCarthy, I.E., and Weigold, E. (1988). *Rep. Prog. Phys.* **51**, 299.
Ritter, A.L., Dennison, J.R., and Dunn, J. (1984*a*). *Rev. Sci. Instrum.* **55**, 1280.
Ritter, A.L., Dennison, J.R., and Jones, R. (1984*b*). *Phys. Rev. Lett.* **53**, 2054.
Weigold, E. (1991). *Aust. J. Phys.* **44**, 277.
Weigold, E., Zheng, Y., and von Niessen, W. (1990). *Chem. Phys.* (in press).
Ziman, J.M. (1971). *J. Phys. C* **4**, 3129.

Manuscript received 14 September, accepted 20 December 1990

